Journal of the Neurological Sciences 399 (2019) 125–139

Contents lists available at ScienceDirect

Journal of the Neurological Sciences

journal homepage: www.elsevier.com/locate/jns

Rapamycin regulates cholesterol biosynthesis and cytoplasmic ribosomal proteins in hippocampus and temporal lobe of APP/PS1 mouse

Xia Wang[a,1], Wenchao Xia[a,1], Kai Li[c,1], Yusheng Zhang[a], Wei Ge[a,*], Chao Ma[b,**]

[a] State Key Laboratory of Medical Molecular Biology, & Department of Immunology, Institute of Basic Medical Sciences Chinese Academy of Medical Sciences, School of Basic Medicine Peking Union Medical College, Beijing, China
[b] Department of Human Anatomy, Histology and Embryology, Institute of Basic Medical Sciences Chinese Academy of Medical Sciences, Neuroscience Center, Chinese Academy of Medical Sciences School of Basic Medicine, Peking Union Medical College, Beijing, China
[c] Department of Neurosurgery, Peking University International Hospital, Peking University, Beijing, China

ARTICLE INFO

Keywords:
Alzheimer's disease
Rapamycin
Cholesterol biosynthesis pathway
Cytoplasmic ribosomal proteins

ABSTRACT

As an inhibitor of the immune system and a longevity drug, rapamycin has been suggested as a treatment for Alzheimer's disease, although the underlying mechanisms remain to be clarified. To elucidate the mechanisms, we performed a high-throughput quantitative proteomics analysis and bioinformatics analysis of the changes in the proteome profiles of hippocampus and temporal lobe of wild-type mice, APP/PS1 mice and rapamycin-treated APP/PS1 mice (ProteomeXchange: PXD009540). Morris Water Maze tests were used to evaluate the effectiveness of rapamycin in APP/PS1 treatment and Western blot analysis was used to verify the proteomics data. The results of Morris Water Maze tests indicated that rapamycin improved the spatial learning and memory abilities of APP/PS1 mice. Proteome analysis identified 100 significantly changed (SC) proteins in hippocampus and 260 in temporal lobe in APP/PS1 mice. Among these, 57 proteins in hippocampus and 167 proteins in temporal lobe were rescued by rapamycin. STRING analysis indicated relatively more complicated protein interactions of AD-related rapamycin rescued proteins in temporal lobe. Pathway analysis showed that SC proteins in APP/PS1 mice were mainly enriched in cholesterol biosynthesis pathway and cytoplasmic ribosomal proteins. After rapamycin treatment, the expression of most proteins in these signaling pathways were reversed. Overall, our findings demonstrate that rapamycin may be an potential strategy which can effectively delays the progression of AD.

1. Introduction

Alzheimer's disease (AD) is a common age-related disorder of the neural system that primarily affects people over the age of 65 years and the occurrence grows with age [1]. AD is characterized by extracellular amyloid plaques deposition and intracellular neurofibrillary tangle formation in the brain [2]. Although AD has been known for > 100 years, the etiology of AD remains to be fully elucidated and there are no drugs that can effectively halt or delay its progression [1,3–5].

Recently, rapamycin attracted the interest of researchers as an immunosuppressive drug that was approved by US FDA (Food and Drug Administration) following successful phase IV clinical trials [6]. Rapamycin can prolong the life-span of yeast, worms, flies, and some mammals, such as mice or monkeys and can also improve the pathological lesion in animal models of AD, such as APP/PS1 mice [7–10]. In humans, the occurrence of AD is closely connected to aging [11]. Rapamycin, which is a targeted inhibitor of rapamycin complex 1 (mTORC1) and a disruptor of rapamycin complex 2 (mTORC2), has been implicated as a treatment for AD and other neurodegenerative disorders [6] [9]. Previous studies indicate that components of the

Abbreviations: Aβ, amyloid β-protein; AD, Alzheimer's disease; APP, amyloid-beta A4 protein; ARR, AD-related rapamycin rescued; BP, biological process; CC, cellular component; CMC-Na, sodium carboxymethyl cellulose; GO, gene ontology; HPLC, High performance liquid chromatography separation; mTORC1, rapamycin complex 1; mTORC2, rapamycin complex 2; mTOR, serine/threonine-protein kinase mTOR; TMT, tandem mass tag; C, significantly changed; PS1, presenilin-1

* Correspondence to: State Key Laboratory of Medical Molecular Biology & Department of Immunology, Institute of Basic Medical Sciences Chinese Academy of Medical Sciences, School of Basic Medicine Peking Union Medical College, Beijing, China.
** Correspondence to: Department of Human Anatomy, Histology and Embryology, Institute of Basic Medical Sciences Chinese Academy of Medical Sciences, Neuroscience Center, Chinese Academy of Medical Sciences School of Basic Medicine, Peking Union Medical College, Beijing, China.
E-mail addresses: wei.ge@chem.ox.ac.uk (W. Ge), machao@ibms.cams.cn (C. Ma).
[1] These authors contributed equally to this work.

https://doi.org/10.1016/j.jns.2019.02.022
Received 10 December 2018; Received in revised form 23 January 2019; Accepted 12 February 2019
Available online 14 February 2019
0022-510X/ © 2019 Elsevier B.V. All rights reserved.

mTOR signaling pathway (upstream: PI3K/Akt, AMPK, MAPK, p53, GTPase, LKB1, ERBB2, IRS-1, PTEN, GSK-3 and insulin/IGF-1; downstream: S6/S6K/p70S6K1, 4EBP1, eIF2 and eIF4E) are involved in AD pathogenesis [12]. The activation of mTOR signaling can induce Aβ generation, which is regulated by several signaling pathways, such as PI3K/AKT/mTOR, GSK-3/mTOR, AMPK/mTOR, insulin/IGF-1/mTOR [12]. In addition, as the key pathway of Aβ degradation, the autophagy/lysosome-dependent clearance of Aβ is regulated by mTOR and mTOR inhibition can enhance Aβ clearance [12]. Moreover, mTOR activation triggers tau hyperphosphorylation and neurofibrillary tangle formation via phosphatase 2A and GSK-3-dependent phosphorylation of tau [12]. Rapamycin has been reported to improve neuronal survival and synapse plasticity to alleviate the symptoms of AD by inhibiting hyperphosphorylation of tau, accumulation of Aβ, aging, oxidative stress, and inflammation and enhancement of autophagy [12–15]. The latest research shows that rapamycin also alters neurovascular functions in ApoE4 transgenic mice and mTOR signaling functions as an autophagic intermediary of the TREM2 mutation and AD pathology [16,17]. Although rapamycin has been identified as a potential treatment for AD, the mechanisms of the therapeutic effect remain to be elucidated.

Medial temporal lobe atrophy has been shown to commence earlier than hippocampus atrophy, occurring 3.5 years (0.7–7.5 years) before disease onset [18]. Usually, the abnormalities associated with AD are first observed in the frontal and temporal lobes and then gradually extend to the hippocampus and other areas of the brain [2]. This discordance indicates that different mechanisms are responsible for the changes in the hippocampus and temporal lobe; however, the molecular differences between these regions remain to be clarified.

High-throughput proteomics analysis based on mass spectrum detection and tandem mass tag (TMT™)-labeling techniques are now widely used for the quantitative analysis of proteins in biological samples [19]. Proteomics analysis can be used to investigate disease pathogenesis, disease biomarkers and treatment targets as well as in evaluation of the efficacy of drugs [20,21]. When combined with genomic ontology, protein interaction networks and pathway analysis, proteomics analysis can be used to provide a comprehensive depiction of the changes associated with diseases at the protein level [21].

APP/PS1 mice, which carry the Swedish mutation of hAPP and the dE9 mutation of PS1 are extensively used in studies of AD pathogenesis, AD treatment and drug development, are models used to investigate the role of Aβ in AD pathogenesis [22,23]. The Swedish mutation of hAPP increases Aβ production by stimulating BACE cleavage, while the dE9 mutation of PS1 increases the ratio of Aβ42/Aβ40, which are initiating factors in dementia, although the subsequent signaling is not clear [23].

Investigations of the mechanism of AD pathogenesis and the functions of rapamycin in AD are of extreme importance. To clarify these mechanisms, we used six-plex isobaric TMT™-labeling proteomics and bioinformatic analysis strategies to detect the alterative protein profiles of wild-type (WT) mice, APP/PS1 mice and rapamycin-treated APP/PS1 mice. Subsequently, STRING and pathway analyses were used to identify the differences between hippocampus and temporal lobe and the key signals associated with APP/PS1 mice and rapamycin therapy. Moreover, the effectiveness of rapamycin in APP/PS1 mice treatment was evaluated by Morris Water Maze tests and the accuracy of the proteomics data was verified by Western blot analysis.

2. Materials and methods

2.1. Reagents

Rapamycin (MedChemexpress, HY-10219/CS-0063, USA); urea, iodoacetamide and dithiothreitol (GE Healthcare, LC, UK); proteinase inhibitor cocktail tablet mini (Roche, BS, CH); TMT™ Mass Tagging Kits (Thermo Scientific, NJ, USA); sequencing-grade trypsin/Lys-C mix (Promega, WI, USA); The Enhanced Chemiluminescence Kit was gained from Millipore (MA) and all the rest of reagents were purchased from Sigma (MO).

2.2. Antibodies

Anti-β-actin (anti-Actb, rabbit-anti-mouse, GTX124123, GeneTeX, CA), anti-farnesyl pyrophosphate synthase (anti-Fdps, rabbit-anti-mouse, 16,129–1-AP, Proteintech Group, Chicago, IL, USA), anti-diphosphomevalonate decarboxylase (anti-Mvd, rabbit-anti-mouse, ab96226, Abcam, Cambridge, UK), anti-hydroxymethylglutaryl-CoA synthase, cytoplasmic (anti-Hmgcs1, rabbit-anti-mouse, ab155787, Abcam, Cambridge, UK), anti-ribosomal protein S6 kinase alpha-2 (anti-Rps6ka2, rabbit-anti-mouse, ab32563, Abcam, Cambridge, UK), anti-60S ribosomal protein L36a (anti-Rpl36a, rabbit-anti-mouse, ab175016, Abcam, Cambridge, UK), anti-40S ribosomal protein S8 (anti-Rps8, rabbit-anti-mouse, ab201454, Abcam, Cambridge, UK), anti-60S ribosomal protein L23a (anti-Rpl23a, rabbit-anti-mouse, Sc-135,388, Santa Cruz, CA, USA).

2.3. Animals

APP/PS1 mice (32 weeks old, 4 male and 3 male, Jackson Laboratory, Bar Harbor, ME, USA, https,//www.jax.org/strain/004462) and background- and age-matched WT mice were housed and bred in specific pathogen-free conditions, which did not carry the retinal degeneration allele *Pde6b*^{rd1}. All experiments complied with the National Institutes of Health Guide for the Care and Use of Laboratory Animals and got the permission of the Association for Assessment and Laboratory Animal Care.

2.4. Morris water maze tests

The spatial learning and memory abilities of WT mice (n = 7, oral administration of 5% CMC-Na (carboxymethylcellulose sodium)), AD mice (APP/PS1 mice, n = 7, oral administration of 5% CMC—Na), and AD-Rapa mice (APP/PS1 mice, n = 7, oral administration of rapamycin 2 mg/kg/day [17], rapamycin dispersed in 5% CMC—Na) were evaluated by Morris Water Maze tests (Fig. 1) [24]. The mice were treated with drug administration for 7 weeks (from 32 to 38 weeks), and Morris Water Maze tests were performed on the 38nd week (Fig. 1A). This test was performed in a circular pool (100 cm diameter) with constant water temperature (20 ± 1 °C). The pool was divided into four equally-sized areas with the escape platform placed in the center of B quadrant during the test. For adaptation training (day 1), two trials were performed per day in which the mouse was allowed to search for the visible escape platform for 60 s (one hour rest per trial). If the mouse failed to find the platform during this period, the mouse was placed on the platform for 20 s. The mouse was dried after every test. During hidden platform training (day 2–7), the platform was submerged in water to approximately 1 cm below the surface and the flag was removed; fat-free dried milk was added to hide the escape platform. Each mouse underwent 4 four trials per day (1 hour rest per trial) for six consecutive days to train them to find the submerged escape platform. If the mouse failed to find the platform, the trial was repeated according to the adaptive training. The mouse was dried after every test. The duration and path efficiency of each trial were monitored and recorded using a video tracking system (ANY-maze, Stoelting Co., Wood Dale, IL, USA). After the training test of day 7, all mice will go on probe test. In probe test, the escape platform was removed and fat-free dried milk was added into pool. The mice were allowed to swim freely in a limited time of 60s and the tracks of all mice were recorded by ANY-maze.

2.5. Hippocampus and temporal lobe tissue isolation

After 40 weeks, mice in each group were sacrificed under deep anesthesia with intraperitoneal injection of pentobarbital sodium. Brains

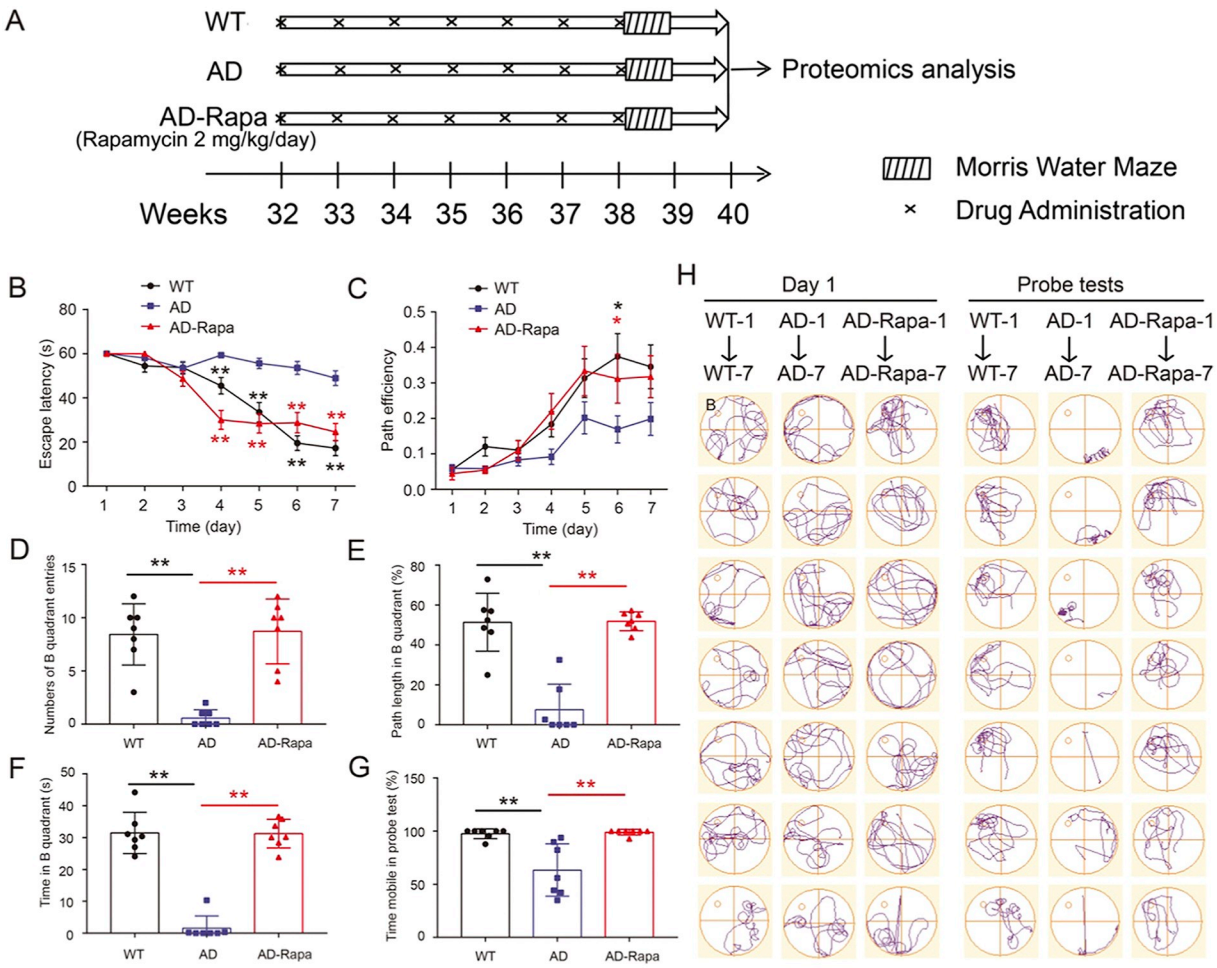

Fig. 1. The spatial learning and memory of APP/PS1 mice were improved by rapamycin treatment. (A) The scheme of rapamycin administration, Morris Water Maze tests and proteomics analysis. (B, C) For Morris Water Maze tests, the escape latency and path efficiency of the different groups (WT, AD, and AD-Rapa) were compared from day 1 to day 7. Data represent the mean ± SEM of 7 animals per group. (D, E, F, G) In probe test, numbers of B quadrant entries, % of path length in B quadrant, time in B quadrant and % of time mobile in probe tests (total time = 60s) were evaluated. Data represent the mean ± SD of 7 animals per group. (H): The movement trail of WT, AD and AD-Rapa mice in day 1 and probe tests were showed above and the platform was put in B quadrant. (The symbol of * means $P < .05$ and ** means $P < .01$, one-way ANOVA: B and C; unpaired two-tailed Student's *t*-test: D, E, F and G).

were carefully removed. Due to the more severely affection of left hemisphere in AD patients compared with right hemisphere [25,26], left hippocampus and left temporal lobe tissues were carefully isolated and immediately frozen at -80 °C. Four mice including 2 male and 2 female were selected in each group for further investigation: WT group, AD group, and AD-Rapa group.

2.6. Proteomic analysis

The proteomic analysis workflow is shown in supplementary fig. 1

2.7. Sample preparation

Proteins were extracted from the hippocampus and temporal lobe tissues by using the liquid nitrogen grinding method as described previously [20,21]. The homogenized tissues were treated with ice-cold lysis buffer (8 M urea and 1 × cocktail in PBS, pH 8.0) and then transferred to a 1.5-mL tube on ice. Cellular debris was removed by centrifugation (12,000 rpm, 15 min, 4 °C) and the supernatant was transferred to a fresh 1.5-mL tube for immediate storage at −80 °C. The protein concentration of the supernatant was determined using the NanoDrop 2000 (Thermo Scientific, NJ, USA) following the manufacturer's instructions.

2.8. TMT-labeling

The protein solutions derived from the WT-hippocampus, AD-hippocampus, AD-Rapa-hippocampus, WT-temporal lobe, AD-temporal lobe and AD-Rapa-temporal lobe groups were used in TMT labeling experiments. For each group, 100 μg proteins pooled from four mice (25 μg /mice) were treated with 10 mM dithiothreitol (1 h, 37 °C) and then incubated with 25 mM iodoacetamide (30 min in the dark at room temperature). The solutions were then diluted with PBS (pH 8.0) to a final urea concentration of 1.0 M and trypsin/Lys-C mix (1100 *w*/w) was added into the reaction tube to digest the proteins to peptides (overnight at 37 °C). Subsequently, 100% trifluoroacetic acid (TFA) was added to each tube to regulate the pH of the peptide solutions at 1–2. After centrifugation (12,000 rpm, 10 min, room temperature), the samples were desalted using a reversed-phase column (Oasis HLB, Waters, MC, USA) according to the manufacturer's protocol. The extracts were vacuum-dried and then dissolved in 50 μL 200 mM triethylammonium bicarbonate buffer. The solutions were centrifuged (12,000 rpm, 2 min) and the supernatants were transferred to new tubes. Subsequently, 40 μL TMT reagents (0.8 mg TMT dissolved in 40 μL acetonitrile) were added to each supernatant and incubated for 1 h at room temperature. Six TMT labels were used to label the different samples: TMT-130, WT-hippocampus; TMT-126, AD-hippocampus; TMT-128, AD-Rapa-hippocampus; TMT-131, WT-temporal lobe; TMT-

127, AD-temporal lobe; TMT-129, AD-Rapa-temporal lobe. The reactions were stopped by incubation with 8 μL 5% hydroxylamine for 20 min. After termination of the reactions, the six labeled samples were mixed and the process of adjusting pH, desalting and drying was repeated as previously described. These labeled peptides were then dissolved in 100 μL TFA (0.1% *w*/w).

2.9. High performance liquid chromatography separation (HPLC)

The TMT-labeled peptides (100 μL in 0.1% TFA) were fractionated by HPLC (UltiMate 3000 UPLC, Thermo Scientific) using an Xbridge BEH300 C18 column (4.6 mm × 250 mm, 2.5 μm, Waters) with the following parameters: phase A, ammonium hydroxide (pH 10.0); phase B, methanol; phase C, acetonitrile (pH 10.0); column temperature, 45 °C; flow rate, 1.0 mL/min; test wavelength of ultra violet detector, 214 nm. Ultimately, all fractions were collected in 48 fresh tubes (1.5 min/tube), dried under vacuum and then dissolved in 20 μL 0.1% TFA for further liquid chromatography (LC)-MS/MS analysis.

2.10. Peptide analysis by LC–MS/MS

The high-throughput LC–MS/MS analyses were performed using the Ultimate 3000 RSLCnano System (Thermo Scientific, NJ, USA) and an interfaced Thermo Q Exactive Benchtop Mass Spectrometer (Thermo Scientific, NJ, USA) to identify different TMT labels and the species of peptides. A silica capillary column (70 μL internal diameter, 150 mm length, Upchurch, Oak Harbor, WA, USA) packed with 5 μL C18 silica resin (300 A°, Varian, Lexington, MA, USA) was used to separate peptides by gradient elution (0.30 μL/min, 120 min). Xcalibur 2.1.2 was used gather the data from the Q Exactive mass spectrometer, with the mode set to data-dependent acquisition mode. After the single full-scan mass spectrum in Orbitrap (60,000 resolution, 400–1800 *m*/z), 10 data-dependent MS/MS scans at 27% normalized collision energy (higher energy C-trap dissociation) were conducted to acquire the fragment mass spectrum. Using the Proteome Discoverer 2.1 software (Thermo Scientific), the MS/MS spectra were compared against the UniProt mouse FASTA database (released on October 21, 2017). The recommended settings were used for the search criteria as follows: FDR = 0.01 (false discovery rate); full tryptic specificity required; no more than two missed cleavages; carbamidomethylation (C, +57.021 Da) and TMT-plex (lysine [K] and any N-terminus), static modifications; oxidation (methionine, M), dynamic modification; precursor ion mass (all MS from Orbitrap mass analyzer) tolerances were set to 10 ppm; fragment ion mass (all MS2 spectra) tolerances were set to 20 mmu; the reporter ion intensities per peptide were used for relative protein quantification; the upregulation threshold was 1.10 and the downregulation threshold was 0.90. Ultimately, the mass spectrometry proteomics data was exported via the PRIDE partner repository to the ProteomeXchange Consortium (dataset identifier PXD009540).

2.11. Bioinformatics analysis

Gene Ontology analysis was used for AD-related rapamycin rescued (ARR) proteins classification using Funrich software. STRING database version 10.0 (http://string-db.org) were used to detect the protein-protein interactions of ARR proteins and the medium confidence threshold set to 0.4. For the Wiki pathway analysis, we used an online WEB-based GEne SeT analysis Toolkit (WebGestalt, Vanderbilt University, Nashville, TN, USA, http://www.webgestalt.org/option.php). Cytoscape (3.6.0) was used for protein mapping to pathways. Volcano plots were generated using R Studio with ggplot2 package.

2.12. Western blot

Western blot was used as a mature protein identification and quantification method to verify the proteomics data. This test was performed according to standard protocols and the protein concentrations of the samples were determined using a NanoDrop 2000 (Thermo Scientific, NJ, USA). The general steps were as follows: 1. The preparation of SDS-PAGE gels: 10% separation gel and 5% stacking gel; 2. Electrophoresis: 80 V in stacking gel and 120 V in separation gel; 3. Transmembrane: 450 nm nitrocellulose membrane and 250 nm polyvinylidene fluoride membrane (< 30 KDa) were used to blotting the proteins; 4. Blocking: 5% nonfat dry milk in TBS-T solution (TBS plus 5% Tween) for 30 min; 5. The incubation of primary antibody: 4 °C overnight and the dilution of primary antibodies was 1:10,000 for Actb, 1:1000 for Fdps, 1:1000 for Mvd, 1:1000 for Rps8, 1:1000 for Rps6ka2, 1:500 for Rpl36a, 1:200 for Rpl23a; 6. The incubation of horseradish peroxidase-conjugated goat-anti-rabbit second antibody: the dilution of second antibody was 1:7500 and the incubation time was 60 min; 7. The rinse of membrane used TBS-T solution; 8. Imaging: Enhanced Chemiluminescence reagents and the image was caught by Tanon-5800 Chemiluminescent Imaging System (Tanon, China).

2.13. Statistical analysis

The Morris Water Maze tests of day 1 to day 7 (mean ± SEM), Morris Water Maze tests of probe tests (mean ± SD) and Western blot data (mean ± SD) were plotted and analyzed by using GraphPad prism 7.0. Unpaired two-tailed Student's *t*-test was used for two group comparison and one-way ANOVA was used for multi-group comparisons. *P*-values < .05 were considered to indicate statistical significance.

3. Results

3.1. Rapamycin-treated APP/PS1 mice showed improvement in spatial learning and memory abilities

To evaluate the efficiency of rapamycin in APP/PS1 mice treatment, we conducted Morris Water Maze tests. The escape latency and path efficiency of the WT, AD, and AD-Rapa (oral rapamycin 2 mg/kg/day, 7 weeks) groups were compared. During the adaptive period (day 1), none of the mice were able to find the platform in 60 s. After the hidden platform training, WT mice were able to find the platform rapidly and efficiently, while mice in the AD group were rarely able to find the platform (Fig. 1B–C), which is consistent with previous reports of other transgenic mice [10]. Improvements in spatial learning and memory capacities were observed in the AD-Rapa group compared to the AD group and the effects approached to those of the WT group (Fig. 1B–C). The differences were statistically significant ($P < .05$). For probe tests, rapamycin obviously improved the numbers of B quadrant entries, the proportion of path length in B quadrant and the time in B quadrant of APP/PS1 mice and the data is same to WT mice (Fig. 1D–F). During probe test, the mobile time of WT mice and AD-Rapa mice apparently surpassed APP/PS1 mice, which suggested that rapamycin may activate APP/PS1 mice (Fig. 1G). The detail tracks were shown in Fig. 1H. All the detailed information are shown in Supplementary Table 1. These results indicated that rapamycin can ameliorate the spatial learning and memory deficit in APP/PS1 mice.

3.2. Characterization of the protein profiles in hippocampus and temporal lobe

To investigate the mechanisms underlying treatment of rapamysin in APP/PS1, we used a HPLC-coupled high-throughput mass spectrometry approach to quantitatively characterize the proteome in hippocampus and temporal lobe. At the 40th week after rapamycin treatment (from 32 to 38 weeks), hippocampus and temporal lobe regions from WT, AD, AD-Rapa groups were subjected to proteomic analysis. With a threshold of FDR < 1%, unique peptide > 2, and confidence score > 10, we identified 5092 proteins (Supplementary Table 2).

Proteins that changed > 1.20 fold and < 0.83 fold were defined as

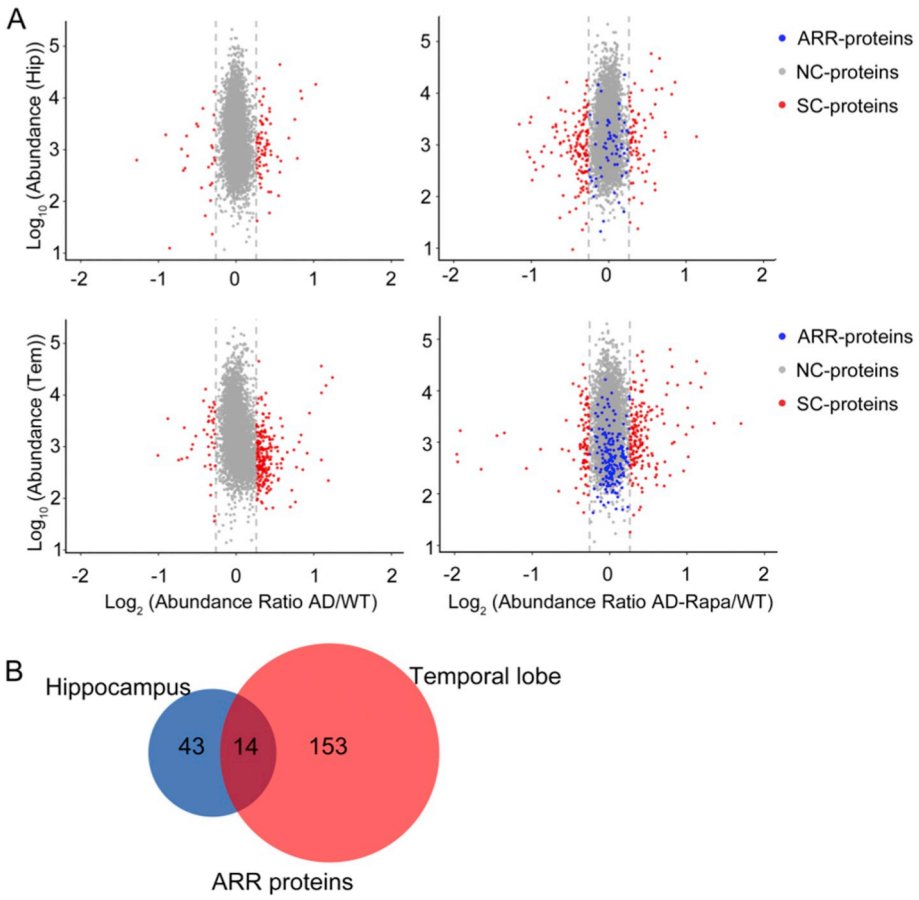

Fig. 2. Characterization of the protein profiles in hippocampus and temporal lobe. (A) Abundance ratios of proteins in hippocampus (Hip) and temporal lobe (Tem). Proteins with a abundance ratio > 1.20 or < 0.83 were defined as significantly changed proteins (SC-proteins) and are represented as red dots. Other proteins were defined as nonsignificantly changed proteins (NC-proteins) and are represented as gray dots. SC-proteins that were restored by rapamycin treatment (AD-related rapamycin rescued proteins, ARR proteins) are represented as blue dots in the right panel. (B) Venn map of ARR proteins in hippocampus and temporal lobe. Fourteen proteins were detected both in hippocampus and in temporal lobe. (For interpretation of the references to colour in this figure legend, the reader is referred to the web version of this article.)

significantly upregulated and downregulated proteins, respectively. We found more significantly changed (SC) proteins in temporal lobe (260 proteins) than hippocampus (100 proteins) (Fig. 2A), which demonstrated more damage in temporal lobe in AD progression, in accordance with earlier atrophy of temporal lobe before disease onset [18]. The AD-related rapamycin rescued (ARR) proteins in APP-PS1 mice were screened in two steps: (1) AD/WT > 1.2-fold or AD/WT < 0.83-fold, (2) 0.83-fold < AD-Rapa/WT < 1.20-fold. After screening, much more proteins in temporal lobe were found rescured with rapamycin treatment, with 57 ARR-proteins in hippocampus and 167 in temporal lobe (Fig. 2A, Table 1). Fourteen overlapped proteins were detected in both regions (Fig. 2B, Table 1).

3.3. Bioinformatics analysis of ARR proteins in hippocampus and temporal lobe

To assess the proteome composition and functional classification of the ARR proteins in hippocampus and temporal lobe, we annotated these proteins to cellular component (CC) and biological process (BP) gene ontology (GO) terms (shown in Fig. 3A). In the hippocampus, most ARR proteins are exosomes (n = 19) and lysosome (n = 15) proteins. While in temporal lobe, a large proportion of proteins were annotated as cytoplasmic proteins (n = 67) and lysosome proteins (n = 36). Most of these ARR proteins in hippocampus and temporal lobe were involved in signal transduction and cell communication process.

STRING analysis of these rapamycin-rescured proteins (Fig. 3B-C) revealed scattered protein-protein interaction among these proteins. Relative more complicated protein interactions were found in temporal lobe. Only 2 ARR proteins, Lnpp5d and H2afy2, were found closely interacted with > 2 proteins in hippocampus. In temporal lobe, Aldh1l2, mt-Nd1, Rpl22, Gm10053, Rab33b, Nt5m, Pde10a, Vps39, Vamp7, and Mog were key network nodes in protein-protein interactions. These results suggested that these proteins may play vital roles in improvement of AD symptom by rapamycin.

Wiki pathway analysis in hippocampus and temporal lobe revealed apparent reversion of proteins expression after rapamycin treatment.

To investigate the effects of rapamycin in APP/PS1 mice, we used the WEB-based GEne SeT analysis Toolkit to further analyze the enriched pathways of the SC proteins in hippocampus and temporal lobe.

Based on Wiki pathway database, we found SC proteins in APP/PS1 mice, compared to WT mice, were mainly enriched in the cholesterol biosynthesis pathway, and cytoplasmic ribosomal proteins. Subsequently, the ratios of proteins identified in the AD/WT (hippocampus), AD/WT (temporal lobe), AD-Rapa/AD (hippocampus) and AD-Rapa/AD (temporal lobe) groups were mapped to these pathways and visualized using Cytoscape (3.6.0).

In the cholesterol biosynthesis pathway (Fig. 4A–4D), Fdps was upregulated in the progression from WT to APP/PS1 mice and were both reversed by rapamycin treatment. In addition, there was no change of Mvk expression in hippocampus of APP/PS1 mice with or without rapamycin treatment; while in the temporal lobe, Mvk was overexpressed in the progression of APP/PS1 pathogenesis, and was inhibited by rapamycin treatment.

A number of cytoplasmic ribosomal proteins (Fig. 5A–5D) participated in AD pathogenesis, and respond to rapamycin treatment. In detail, among the proteins involved in AD pathogenesis, Rpl6, Rpl7, Rpl18, Rpl24, Rpl36a, Rps6 and Rps8 were markedly upregulated in the hippocampus, while Rpl13 and Rpl28 were striking downregulated. In contrast, significantly high levels of Rpl7, Rpl22, Rpl27, Rpl36a, Rps6ka2, and Rps27a and low level of Rps23 were found in the temporal lobe. After rapamycin treatment, in hippocampus, most proteins in the hippocampus were downregulated. In the temporal lobe, widespread inhibition effects were also detected with rapamycin treatment. Changes in the AD pathogenesis-associated proteins, such as Rpl36a,

Table 1
ARR proteins in hippocampus and temporal lobe.

Accession	Gene Name	AD/WT_ Hip	AD-Rapa/WT _Hip	Group	AD/WT_ Tem	AD-Rapa/WT _Tem	Group
Q91X72	Hpx	0.703	0.847	ARR	0.821	0.881	ARR
Q9CWR0	Arhgef25	0.760	1.095	ARR	0.824	1.123	ARR
P62897	Cycs	0.823	0.909	ARR	0.762	0.962	ARR
P43276	Hist1h1b	1.301	1.120	ARR	0.672	1.083	ARR
P10922	H1f0	1.258	1.095	ARR	0.785	0.933	ARR
P43275	Hist1h1a	1.278	1.069	ARR	0.787	0.912	ARR
Q9Z2H2	Rgs6	1.256	1.004	ARR	0.809	1.034	ARR
Q06335	Aplp2	1.208	1.049	ARR	1.225	1.191	ARR
Q920E5	Fdps	1.319	0.997	ARR	1.275	1.051	ARR
Q91YY4	Atpaf2	1.258	1.030	ARR	1.287	0.969	ARR
Q6PGD0	Atraid	1.220	1.104	ARR	1.318	1.129	ARR
P01867	Igh-3	1.201	0.888	ARR	1.354	1.032	ARR
P55065	Pltp	1.448	0.994	ARR	1.579	1.036	ARR
Q9DC29	Abcb6	1.348	1.145	ARR	1.698	0.862	ARR
Q8CBF3	Ephb1	0.553	0.929	ARR	0.917	1.200	
P04186	Cfb	0.735	0.891	ARR	0.932	1.129	
E9Q557	Dsp	0.795	0.937	ARR	1.010	0.634	
Q99JP6	Homer3	0.804	1.013	ARR	1.035	1.751	
Q3TBL6	Tnfaip8l3	0.807	0.847	ARR	1.224	0.794	
Q0VE82	Cpne7	0.821	1.097	ARR	1.017	0.830	
Q3UHB8	Ccdc177	0.822	0.903	ARR	0.958	0.947	
P01899	H2-D1	1.203	1.182	ARR	1.230	1.309	
Q7M729	Scn4b	1.206	0.954	ARR	0.951	0.919	
Q8K012	Fnbp1l	1.208	1.017	ARR	0.954	0.981	
Q8CCK0	H2afy2	1.211	0.970	ARR	1.010	1.069	
O08807	Prdx4	1.219	1.080	ARR	1.097	1.047	
P29416	Hexa	1.219	1.191	ARR	1.204	1.270	
Q78WH7	Camk2n2	1.222	1.067	ARR	0.896	0.904	
O35454	Clcn6	1.224	1.128	ARR	1.369	1.262	
P46660	Ina	1.228	1.154	ARR	1.177	1.358	
O70340	Nptx2	1.233	0.983	ARR	1.073	0.939	
Q9JMB8	Cntn6	1.234	1.055	ARR	1.059	0.943	
Q8BLU0	Flrt2	1.238	0.858	ARR	0.845	0.838	
P97326	Cdh6	1.238	0.892	ARR	0.976	0.984	
Q9CQW2	Arl8b	1.241	1.099	ARR	1.336	1.274	
Q8BP67	Rpl24	1.243	1.069	ARR	1.040	0.947	
Q8JZW4	Cpne5	1.255	1.005	ARR	0.920	0.950	
Q07797	Lgals3bp	1.257	1.126	ARR	1.814	1.521	
Q80TL4	Phf24	1.259	1.094	ARR	1.075	1.054	
P47758	Srprb	1.262	0.996	ARR	1.031	1.006	

(*continued on next page*)

Table 1 (*continued*)

P28867	Prkcd	1.263	0.987	ARR	0.898	1.097	
Q8R420	Abca3	1.281	1.080	ARR	1.509	1.289	
O35526	Stx1a	1.285	0.934	ARR	0.940	0.836	
Q8BYW1	Arhgap25	1.288	0.977	ARR	1.043	1.092	
Q9EQG7	Enpp5	1.294	1.149	ARR	1.445	1.316	
Q91VK4	Itm2c	1.303	1.174	ARR	1.510	1.297	
P63054	Pcp4	1.307	0.992	ARR	1.153	1.042	
Q01149	Col1a2	1.310	0.928	ARR	2.140	2.022	
Q9CR57	Rpl14	1.315	1.121	ARR	0.924	0.861	
Q99JH7	Clstn3	1.321	1.041	ARR	1.312	1.258	
O70551	Srpk1	1.337	0.873	ARR	1.125	0.974	
P63089	Ptn	1.341	0.957	ARR	1.121	1.068	
P14148	Rpl7	1.360	1.151	ARR	1.159	1.150	
Q8BHB9	Clic6	1.362	1.179	ARR	1.014	0.807	
Q99K30	Eps8l2	1.364	1.051	ARR	0.883	1.426	
Q9ES52	Inpp5d	1.478	1.168	ARR	1.714	1.334	
Q6PGH1	Bud31	1.728	0.841	ARR	0.949	0.953	
Q60771	Cldn11	1.124	1.083		0.751	0.975	ARR
Q9D2P8	Mobp	1.045	0.883		0.784	0.996	ARR
P63082	Atp6v0c	1.007	0.781		0.794	1.010	ARR
Q8BW22	Ss18l1	1.010	0.977		0.797	0.871	ARR
Q8BTR5	Dusp28	0.969	1.038		0.798	0.971	ARR
Q8VEA4	Chchd4	0.940	1.108		0.799	0.996	ARR
Q14BI2	Grm2	0.869	0.837		0.801	0.899	ARR
Q9D023	Mpc2	0.897	0.846		0.801	0.939	ARR
Q9CPU4	Mgst3	1.041	0.931		0.807	0.880	ARR
Q61885	Mog	1.013	0.996		0.812	0.980	ARR
Q8BLE7	Slc17a6	1.131	0.910		0.816	0.899	ARR
P60824	Cirbp	0.962	1.083		0.818	1.040	ARR
P12787	Cox5a	0.961	1.052		0.819	1.018	ARR
Q62241	Snrpc	0.949	1.016		0.823	0.891	ARR
O54829	Rgs7	0.990	0.988		0.827	0.935	ARR
P15864	Hist1h1c	1.349	1.209		0.828	0.986	ARR
P53702	Hccs	0.911	0.968		0.828	0.996	ARR
P03888	Mtnd1	0.934	0.930		0.830	0.968	ARR
Q91ZP9	Necab2	0.893	1.034		1.200	0.852	ARR
Q99NH0	Ankrd17	1.028	0.935		1.200	0.987	ARR
Q8VDH1	Fbxo21	0.996	0.992		1.202	0.986	ARR
F6W8I0	Yjefn3	1.180	1.133		1.202	1.172	ARR
Q9DB50	Ap1s2	1.022	0.965		1.203	1.036	ARR
Q8C726	Btbd9	1.048	1.202		1.204	0.923	ARR
Q9QZI8	Serinc1	1.096	1.015		1.204	1.046	ARR
Q6AXF6	Sidt1	1.081	0.977		1.204	1.053	ARR
Q8BVF2	Pdcl3	1.100	1.175		1.205	1.175	ARR

(*continued on next page*)

Table 1 (*continued*)

P49446	Ptpre	0.941	1.002	1.206	0.981	ARR
Q8BTJ4	Enpp4	1.100	1.120	1.206	1.134	ARR
Q924S7	Spred2	0.936	0.935	1.208	1.044	ARR
P46662	Nf2	1.120	0.945	1.210	0.968	ARR
Q8K1S2	Unc5d	1.026	0.946	1.210	0.983	ARR
P70444	Bid	0.970	0.977	1.210	0.994	ARR
O88951	Lin7b	1.029	0.953	1.210	1.031	ARR
Q8VEH3	Arl8a	1.157	1.056	1.210	1.195	ARR
P09470	Ace	1.167	0.988	1.211	0.990	ARR
Q8CII2	Cdc123	1.071	0.987	1.211	1.075	ARR
Q9D0L4	Adck1	1.040	0.982	1.213	1.029	ARR
P83882	Rpl36a	1.260	0.825	1.215	0.966	ARR
O35963	Rab33b	1.040	0.999	1.215	0.995	ARR
Q3U0S6	Rasip1	0.900	0.888	1.215	1.050	ARR
Q6P8M1	Tatdn1	1.017	0.993	1.216	1.022	ARR
Q6PHS6	Snx13	0.946	0.975	1.217	1.001	ARR
Q04899	Cdk18	1.071	0.925	1.218	0.931	ARR
Q91WZ8	Dtnbp1	0.947	1.061	1.218	0.976	ARR
P47746	Cnr1	1.037	0.912	1.219	1.009	ARR
Q8BXK9	Clic5	1.005	0.907	1.219	1.015	ARR
Q5KU39	Vps41	1.081	1.079	1.219	1.097	ARR
P55088	Aqp4	1.092	1.122	1.219	1.130	ARR
Q3U2P1	Sec24a	1.037	1.022	1.220	0.986	ARR
Q811Q9	Pcyt1b	0.957	0.934	1.221	0.919	ARR
O35710	Noct	1.004	1.002	1.221	0.938	ARR
Q3TTA7	Cblb	0.982	0.946	1.221	0.970	ARR
Q8R2R3	Aagab	1.040	0.997	1.221	1.117	ARR
Q8K370	Acad10	1.032	1.037	1.224	1.121	ARR
P70280	Vamp7	1.061	1.088	1.224	1.132	ARR
P56960	Exosc10	0.975	0.998	1.226	0.884	ARR
Q60575	Kif1b	1.002	1.001	1.226	0.940	ARR
Q8BS39	Ccdc32	0.973	0.939	1.226	1.023	ARR
Q8VEH6	Cbwd1	0.939	0.911	1.228	0.978	ARR
Q8BYI8	Fam234b	0.965	0.920	1.229	0.977	ARR
Q9CPT5	Nop16	1.022	0.973	1.232	1.129	ARR
Q8CIP4	Mark4	0.842	0.965	1.233	0.956	ARR
Q08024	Cbfb	1.030	1.078	1.235	1.106	ARR
Q8BH64	Ehd2	1.018	1.047	1.235	1.155	ARR
Q8CBX0	Tmem63c	1.086	0.991	1.236	0.989	ARR
Q3UMF0	Cobll1	1.141	0.961	1.236	1.013	ARR
Q00915	Rbp1	1.148	0.968	1.237	1.025	ARR
Q8VCV1	Abhd17c	0.871	0.973	1.241	1.031	ARR
Q3UFY8	Trmt10c	0.941	0.665	1.244	1.003	ARR
P61358	Rpl27	1.067	0.752	1.245	0.895	ARR

(*continued on next page*)

Table 1 (*continued*)

Q7TSK2	Sez6	1.045	1.041	1.246	0.973	ARR
Q80UU9	Pgrmc2	0.991	0.900	1.247	0.948	ARR
Q8BPG6	Sumf2	0.980	0.987	1.247	1.023	ARR
A3KFX0	Nt5c1a	1.041	1.074	1.247	1.108	ARR
Q8CCF0	Prpf31	1.082	1.018	1.249	1.100	ARR
Q9JIQ3	Diablo	1.180	1.036	1.249	1.129	ARR
Q61823	Pdcd4	1.004	1.498	1.250	1.144	ARR
Q8BLV3	Slc9a7	1.058	0.969	1.251	1.005	ARR
Q91VH1	Adipor1	1.113	1.032	1.253	0.988	ARR
P67984	Rpl22	0.882	0.647	1.256	0.957	ARR
Q8VCE6	Nt5m	0.991	1.067	1.256	1.071	ARR
Q08890	Ids	1.091	1.181	1.256	1.075	ARR
E9Q5C9	Nolc1	1.205	0.790	1.257	0.925	ARR
Q3UGY8	Arfgef3	1.185	1.060	1.257	1.190	ARR
Q05186	Rcn1	1.187	1.216	1.259	0.910	ARR
P58069	Rasa2	1.082	1.048	1.261	1.067	ARR
Q9JIS8	Slc12a4	1.036	1.016	1.263	0.948	ARR
Q9WUK6	Zbtb18	1.038	0.902	1.265	0.999	ARR
Q8BKU8	Tmem87b	0.992	0.952	1.265	1.022	ARR
Q9CWQ0	Dph5	0.994	0.993	1.268	0.981	ARR
E1U8D0	Soga1	0.982	0.959	1.268	1.000	ARR
Q80V26	Impad1	0.969	0.990	1.269	1.037	ARR
Q9WVI9	Mapk8ip1	1.107	1.056	1.270	1.082	ARR
Q9EQS9	Igdcc4	1.017	0.955	1.271	0.997	ARR
P01837	Igkc	1.127	0.758	1.272	0.969	ARR
P70445	Eif4ebp2	1.011	1.158	1.273	1.048	ARR
Q641K1	Agtpbp1	1.053	0.967	1.274	0.961	ARR
Q9Z1M7	Large1	1.028	0.983	1.274	1.073	ARR
Q9Z275	Rlbp1	1.091	1.016	1.274	1.073	ARR
Q3UHK1	Slc2a13	1.122	0.928	1.275	0.992	ARR
Q921C5	Bicd2	1.058	1.012	1.276	1.034	ARR
Q61730	Il1rap	0.966	1.056	1.277	1.109	ARR
O70200	Aif1	1.157	1.123	1.278	1.129	ARR
P62046	Lrch1	0.977	0.964	1.283	1.026	ARR
Q8K009	Aldh1l2	1.117	1.127	1.284	1.158	ARR
Q8BXC6	Commd2	1.042	1.146	1.285	0.947	ARR
P98195	Atp9b	1.126	1.017	1.285	1.013	ARR
Q8BQ47	Cnpy4	1.055	1.082	1.285	1.098	ARR
Q9R008	Mvk	1.038	1.056	1.286	1.007	ARR
Q62313	Tgoln1	1.055	0.954	1.288	1.021	ARR
Q68FE2	Atg9a	1.090	0.935	1.289	1.118	ARR
Q9JJZ4	Ube2j1	1.023	1.004	1.293	0.940	ARR
Q9Z103	Adnp	0.952	0.922	1.295	0.939	ARR
P20065	Tmsb4x	0.940	0.897	1.296	0.954	ARR

(*continued on next page*)

Table 1 (*continued*)

Q3UH99	Shisa6	0.858	0.962	1.297	0.962	ARR
Q91W40	Klc3	1.001	1.075	1.300	1.109	ARR
Q3UFQ8	Carmil3	1.017	0.942	1.303	1.036	ARR
Q9ET22	Dpp7	1.175	1.046	1.304	1.192	ARR
O70496	Clcn7	1.168	1.071	1.307	0.969	ARR
Q8R4C2	Rufy2	1.173	1.031	1.307	1.097	ARR
Q14AX6	Cdk12	1.164	0.946	1.308	1.059	ARR
Q61220	Nell2	1.084	1.116	1.308	1.162	ARR
E9PZM4	Chd2	1.010	1.022	1.311	1.021	ARR
Q9JI99	Sgpp1	1.043	0.783	1.313	0.943	ARR
Q8K296	Mtmr3	1.013	0.943	1.315	0.998	ARR
Q8BTU1	Cfap20	1.094	1.079	1.316	1.069	ARR
P97333	Nrp1	0.891	1.031	1.317	0.959	ARR
Q6P6M7	Sepsecs	0.993	0.935	1.318	0.919	ARR
O09044	Snap23	1.066	1.034	1.319	1.040	ARR
Q8BGT5	Gpt2	1.087	1.144	1.327	1.115	ARR
P41233	Abca1	1.001	1.092	1.331	1.066	ARR
Q9WUH1	Tmem115	1.085	0.948	1.336	0.964	ARR
Q8R0G7	Spns1	1.078	1.020	1.337	1.121	ARR
P50294	Nat1	0.987	1.072	1.339	1.019	ARR
Q6P5D4	Cep135	1.119	1.077	1.341	1.020	ARR
Q9D187	Fam96b	1.043	1.062	1.341	1.026	ARR
Q8BPB0	Mob1b	0.940	0.923	1.343	1.001	ARR
Q6PDC0	Rundc3b	1.142	1.078	1.343	1.123	ARR
Q9D753	Exosc8	0.980	1.010	1.348	0.967	ARR
Q9JMA2	Qtrt1	0.978	1.053	1.358	1.024	ARR
Q8BUR3	Foxj3	1.090	0.979	1.362	0.976	ARR
Q8BKG3	Ptk7	1.177	0.945	1.365	1.011	ARR
Q8R5L3	Vps39	1.165	1.041	1.367	1.125	ARR
Q60809	Cnot7	0.947	1.116	1.373	1.092	ARR
Q64299	Nov	1.199	0.928	1.374	0.838	ARR
P42703	Lifr	1.023	0.958	1.389	1.176	ARR
Q60841	Reln	1.018	0.979	1.399	1.085	ARR
Q9CQ33	Lztr1	1.109	1.041	1.461	0.920	ARR
Q8VCN5	Cth	0.979	0.963	1.491	0.961	ARR
Q9Z0S9	Rabac1	1.044	0.952	1.676	1.011	ARR
Q8CA95	Pde10a	0.991	0.916	1.756	0.895	ARR
Q9DCC8	Tomm20	1.101	0.975	2.278	0.897	ARR

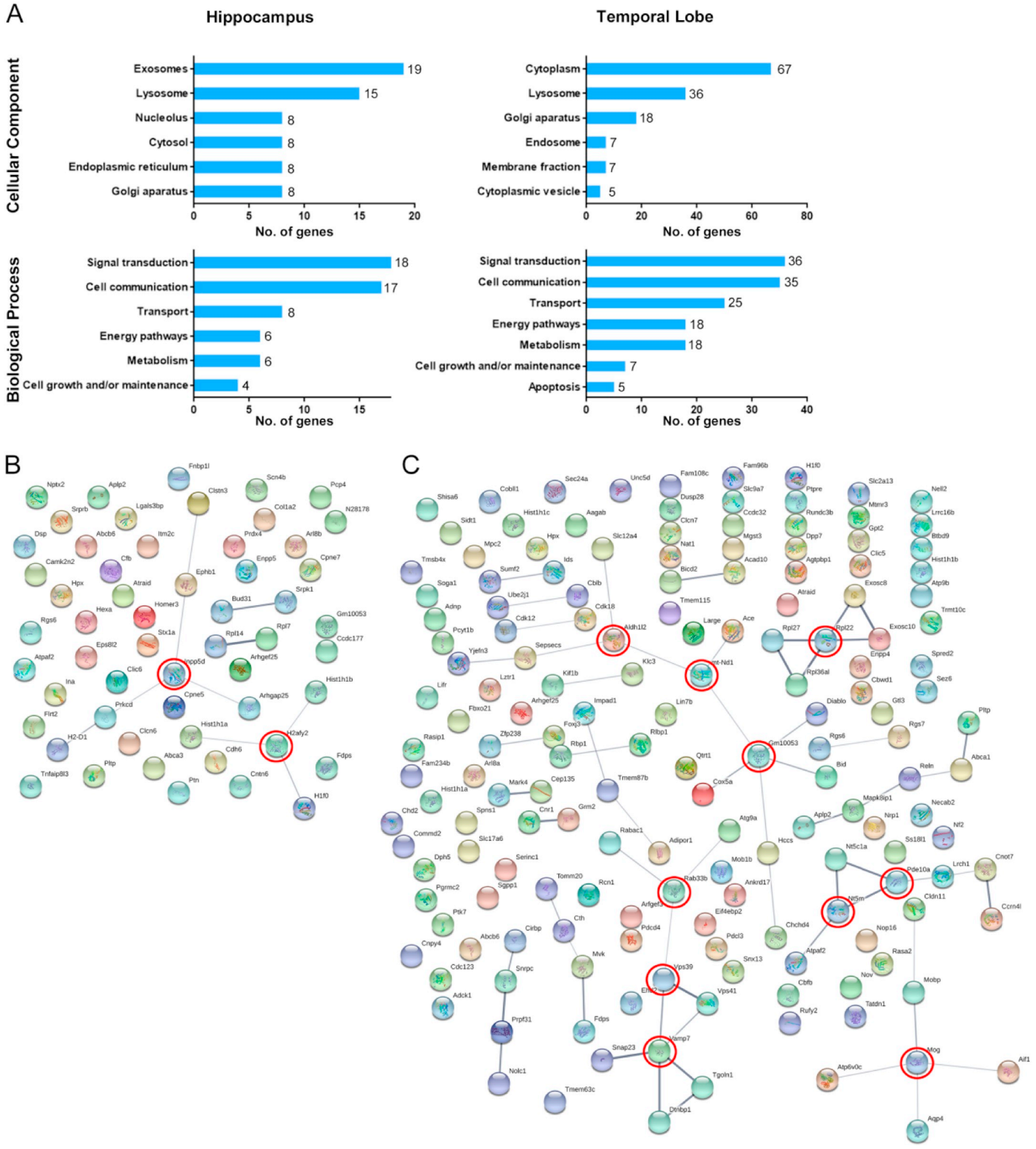

Fig. 3. Bioinformatic analysis of ARR proteins in hippocampus and temporal lobe. (A) GO analysis. (B,C) STRING analysis. Scattered protein-protein interactions were found among these ARR proteins. (B) ARR proteins in hippocampus. Only 2 proteins were found interacted with > 2 proteins. (C) ARR proteins in temporal lobe. Ten proteins were detected interacted with > 2 proteins.

Rps8, Rpl22, Rpl27, and Rps6ka2, were reversed by rapamycin.

Overall, rapamycin may play a regulatory role in APP/PS1 pathogenesis via its effects on the cholesterol biosynthesis pathway, and cytoplasmic ribosomal proteins.

3.4. Western blot verification

To verify the reliability of our proteomics data, Fdps, Mvd, Rpl36a, Rpl23a, Rps8 and Rps6ka2 were selected for western blot analysis using Actb as the background reference. The results showed the same trend as

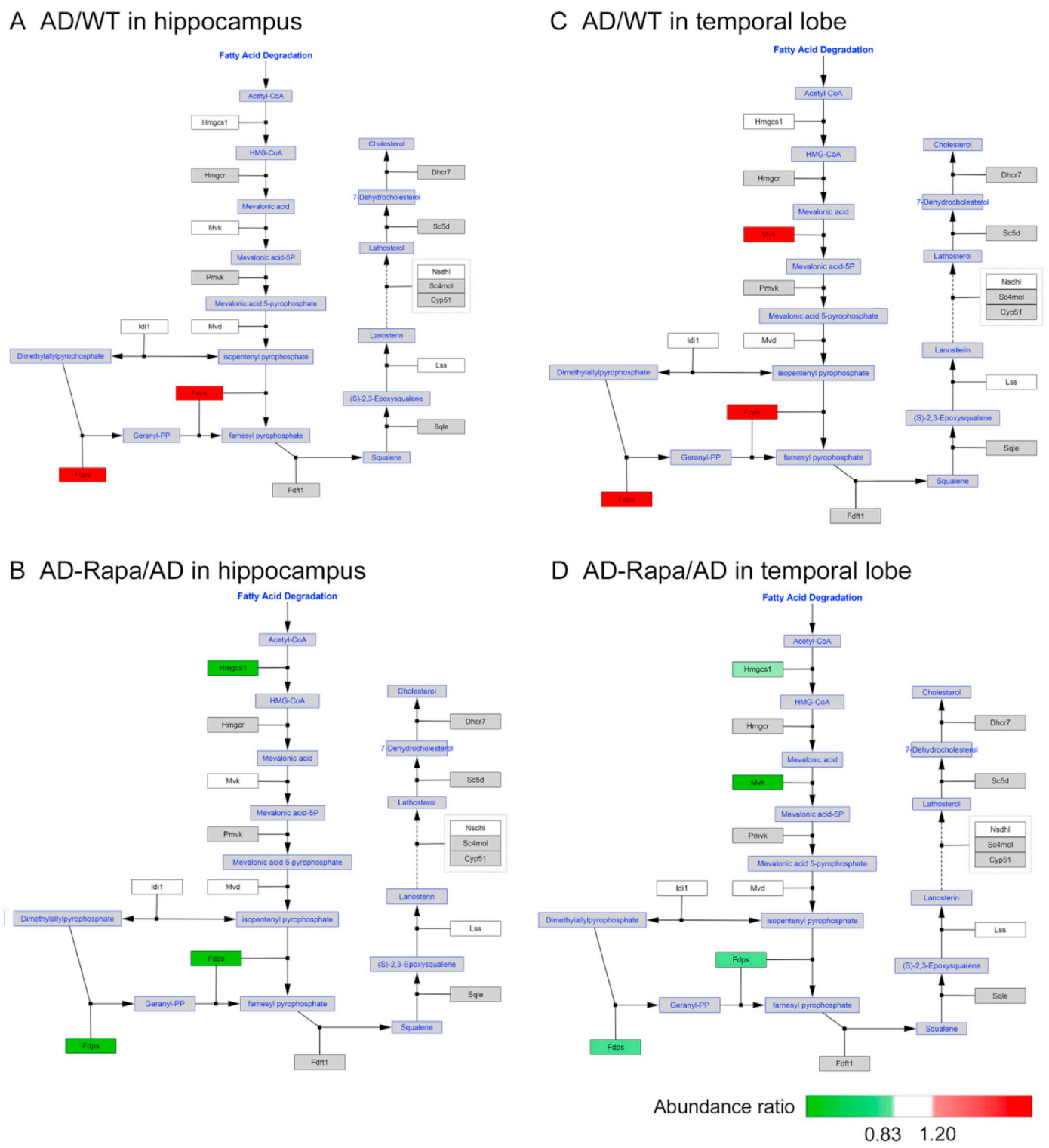

Fig. 4. The differentially expressed proteins in the Wiki pathway of cholesterol biosynthesis pathway. Proteins are represented as boxes and labeled with the gene names. Relative protein expression level is indicated by colors: red indicates upregulation and green indicates downregulation. Gray indicates that the proteins were not identified in this study. (For interpretation of the references to colour in this figure legend, the reader is referred to the web version of this article.)

data obtained in the proteomics analysis (Fig. 6), as well as the differences were statistically significant ($P < .05$). In the hippocampus, Fdps and Rps8 were upregulated from WT to APP/PS1 and were downregulated by rapamycin. Similarly, in temporal lobe, Fdps and Rpl36a were upregulated from WT to APP/PS1 and were downregulated by rapamycin. That is, rapamycin may alleviate AD symptom through the regulation of cholesterol biosynthesis pathway and ribosomal proteins including Fdps and Rps8 in hippocampus and Fdps and Rpl36a in the temporal lobe.

Some pivotal proteins, including Pltp, Inpp5d, Col1a2, Vtn and Plcg2 were selected for analysis of their secondary mass spectrum (Supplementary Fig. 2). The peaks of precursor ions, product ions and TMT tags were detected by LC–MS/MS and the specific sequences of these peptides were generated by spectral analysis.

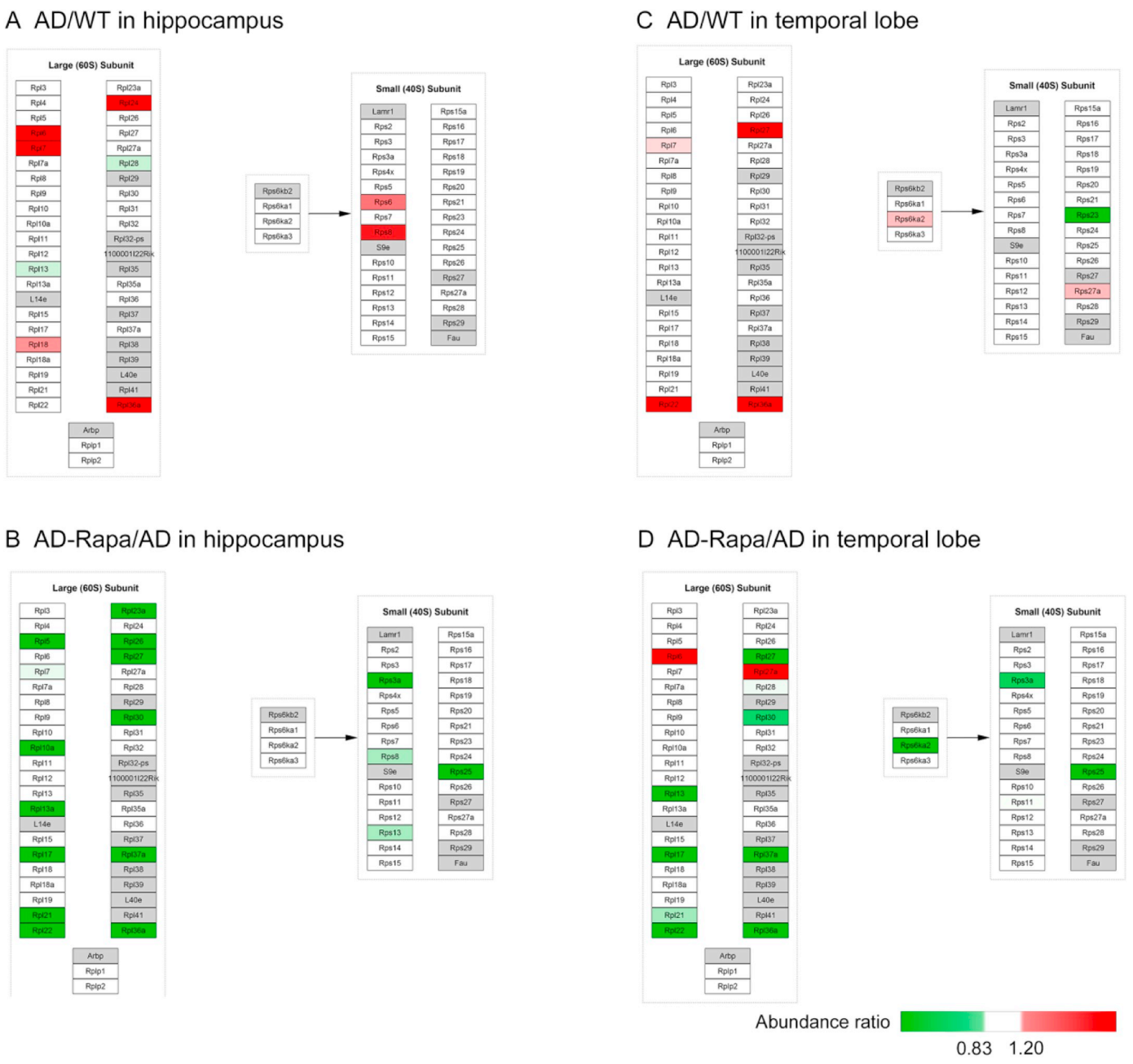

Fig. 5. The differentially expressed proteins in the Wiki pathway of cytoplasmic ribosomal proteins. Proteins are represented as boxes and labeled with the gene names. Relative protein expression level is indicated by colors: red indicates upregulation and green indicates downregulation. Gray indicates that the proteins were not identified in this study. (For interpretation of the references to colour in this figure legend, the reader is referred to the web version of this article.)

4. Discussion

In this study, we found that rapamycin can ameliorate the spatial learning and memory deficit in APP/PS1 mice. TMT-labeled quantitative proteome analysis revealed more SC proteins in temporal lobe than hippocampus. Also, more SC proteins were rescued by rapamycin in temporal lobe, with 57 ARR-proteins in hippocampus and 167 in temporal lobe. STRING analysis indicated relatively more complicated protein interactions of ARR proteins in temporal lobe. Pathway analysis showed that SC proteins in APP/PS1 mice were mainly enriched in cholesterol biosynthesis pathway, and cytoplasmic ribosomal proteins. After rapamycin treatment, the expression of most proteins in these signaling pathways were reversed.

The Morris Water Maze test is frequently used in the evaluation of the memory and learning damage in AD model mouse [24]. In accordance with previous reports, we demonstrated the protective effects of rapamycin in the APP/PS1 model mouse [10]. Rapamycin successfully relieved the symptoms and improved the memory and learning abilities of APP/PS1 mice, indicating that rapamycin may be effective in treating various phenotypic aspects of AD.

It was reported that human AD and mild cognitive impairment postmortem brain samples showed high mTOR activation compared to healthy controls [27]. In an AD mouse model, a global inhibition of mTOR signaling with rapamycin reduced cognitive deficts [28]. Rapamycin is a targeted inhibitor of mTORC1, and a disruptor of mTORC2. Our results in APP/PS1 mice also demonstrated the improvement of spatial learning and memory by rapamycin. Furthermore, Neelam et al. reported that depletion of mTOR activator Rheb in forebrain can elicits spatial memory deficits in mice [29]. Based on these results, we speculate that regulation of mTOR signaling may play vital roles in

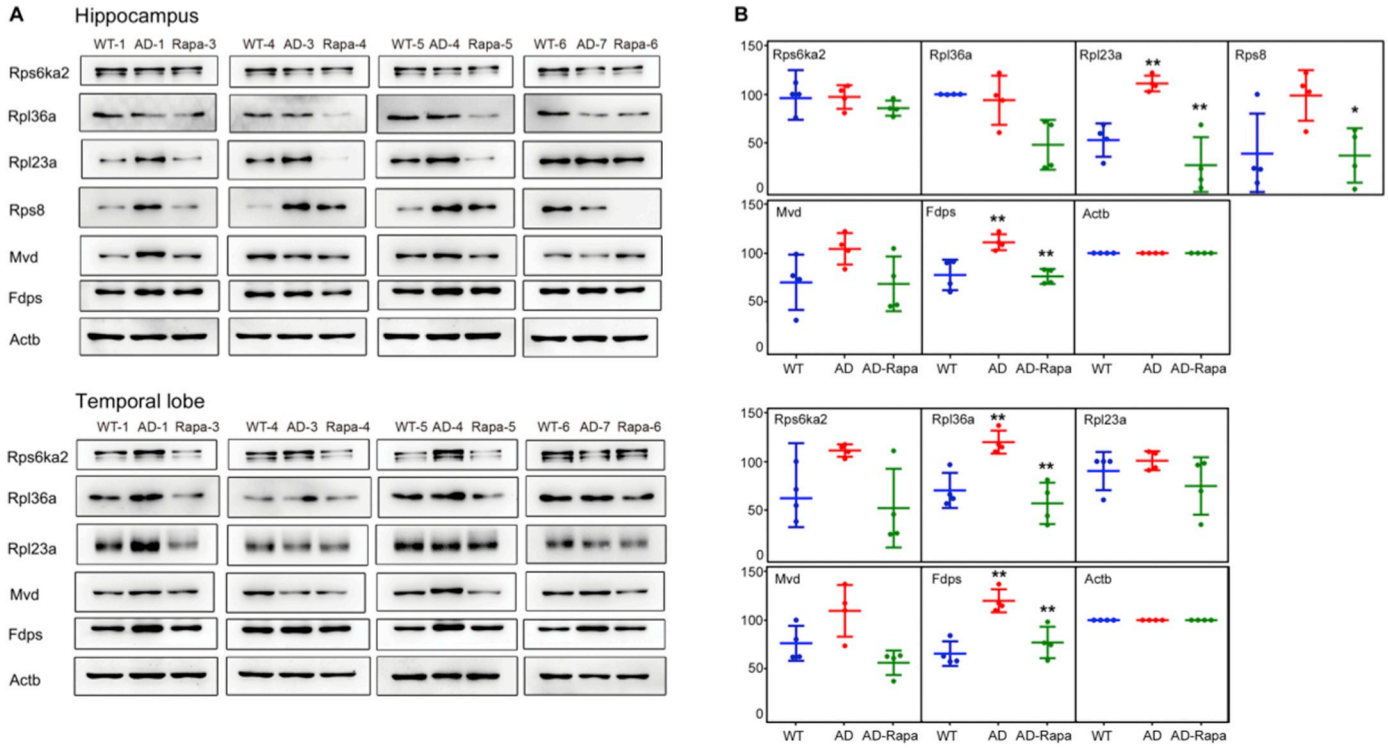

Fig. 6. Western blot verification of MS analysis. (A) Verification of Rps6ka2, Rpl36a, Rpl23a, Rps8, Mvd, Fdps and Actb in hippocampus and temporal lobe. (B) The statistical analysis of the gray-scale value of proteins in hippocampus and temporal lobe. Data represent the mean ± SD of each group ($n = 4$). The symbol of * means $P < .05$ and ** means $P < .01$.

ameliorating memory deficits in AD.

It has been reported that lipid metabolism controls the occurrence of AD by regulating the synthesis, aggregation, neurotoxicity and elimination of Aβ and the phosphorylation of tau, as well as cerebral vessel dysfunction [30]. ApoE and cholesterol metabolism dysfunctions are the center of the lipid metabolism abnormalities hypothesis [30]. As a pathological chaperone of Aβ, ApoE is an important transporter of cholesterol and other lipids among CNS cells and is also a vital regulator of cholesterol metabolism [30,31]. ApoE4, with lower cholesterol transport ability, is associated with the highest risk to human AD and higher levels of oligomeric Aβ, which create neurotoxins and stimulate tau phosphorylation [31,32]. It is also reported that abnormal cholesterol levels are a sensitive indicator of Aβ production, amyloid genesis, tau phosphorylation and tau proteolysis [31,33]. As an important recent study reported, cholesterol plays a specific catalytic role in the aggregation of Aβ42 [34]. Cholesterol is also essential for axonal growth and synaptic formation and remodeling as well as the memory generation and learning [31,33]. Interestingly, inhibiting the synthesis of cholesterol can prevent AD and cardiovascular disease [31]. Previous studies of European samples revealed that cholesterol-related genes, such as HMGCS2 and FDPS were associated with sporadic AD [35]. In addition, the expression of cholesterol metabolism genes, including Fdps, Mvk and Mvd, were regulated by oligomeric amyloid-β peptides [36]. Furthermore, Pltp which cooperates with Abca1 to regulate cholesterol efflux, was found as the rapamycin targeted proteins [37]. It is reported that the level of human PLTP is increased and can alter APP processing and amyloid-β metabolism to affect learning and memory abilities in mouse models [38,39]. Intriguingly, in our study, rapamycin suppressed cholesterol biosynthesis regulators, including Fdps and Mvk. The effects of rapamycin are so wide-ranging that it may be the key to the treatment of AD.

Ribosomal dysfunctions such as decreased protein synthesis capacity, reduced levels of ribosomal RNA and tRNA and increased RNA oxidation are regarded as an early event in AD [40,41]. High levels of ribosomal S6 kinase 1 (Rps6k1) are found in the AD brain and suppression of Rps6k1 expression improves spatial memory capacity and synaptic plasticity in an AD model mouse through the inhibition of Aβ and tau accumulation [42]. Furthermore, Rps6k1 inhibition increases the lifespan of some nematodes and mammals [42]. Furthermore, ribosomal assembly as well as RNA transcription and protein synthesis are regulated by mTORC1 [43]. A recent study revealed that ribosome proteins, such as Rpl7 and Rpl26, are associated with mTOR2 activation, which is promoted by insulin-stimulated PI3K signaling [44]. Based on the results of our study, the inhibition of mTOR by rapamycin reversed ribosomal proteins such as Rps6ka2 that play significant roles in APP/PS1 pathogenesis or mTOR regulation. Moreover, serious ribosomal dysfunctions are found in APP/PS1 mice as well as these dysfunctions are inhibited by rapamycin. Therefore we may deduce that early rapamycin interference in AD may prevent or delay the progression of AD.

In combination, these findings strongly implicate rapamycin as a potential treatment strategy in AD pathogenesis.

5. Conclusions

The findings of our study indicate that rapamycin effectively ameliorate the spatial learning and memory deficit in APP/PS1 mice, and rapamycin treatment rescued the protein expression in cholesterol biosynthesis pathway, and cytoplasmic ribosomal proteins. Our results provide important insights into the etiology of AD pathogenesis and the mechanism of rapamycin treatment, which pave a way for further clinical use of rapamycin.

Supplementary data to this article can be found online at https://doi.org/10.1016/j.jns.2019.02.022.

Acknowledgements

This work was supported by grants from the National Natural

Science Foundation of China (NSFC #81801180, #91632113), the Shanghai Brain-Intelligence Project from STCSM (16JC1420500, 16JC1420502), the CAMS Innovation Fund for Medical Sciences (CIFMS #2017-I2M-3-008).

Competing interests

The authors have declared no conflict of interest

References

[1] A.s, Association, 2018 Alzheimer's disease facts and figures, Alzheimers Dement. 14 (3) (2018) 367–429.
[2] C.L. Masters, R. Bateman, K. Blennow, C.C. Rowe, R.A. Sperling, J.L. Cummings, Alzheimer's disease, Nat. Rev. Dis. Primers. 1 (2015) 15056.
[3] P. Scheltens, K. Blennow, M.M. Breteler, B. de Strooper, G.B. Frisoni, S. Salloway, W.M. Van der Flier, Alzheimer's disease, Lancet 388 (10043) (2016) 505–517.
[4] W.V. Graham, A. Bonito-Oliva, T.P. Sakmar, Update on Alzheimer's disease therapy and prevention strategies, Annu. Rev. Med. 68 (2017) 413–430.
[5] R.S. Doody, R.G. Thomas, M. Farlow, T. Iwatsubo, B. Vellas, S. Joffe, K. Kieburtz, R. Raman, X. Sun, P.S. Aisen, E. Siemers, H. Liu-Seifert, R. Mohs, Phase 3 trials of solanezumab for mild-to-moderate Alzheimer's disease, N. Engl. J. Med. 370 (4) (2014) 311–321.
[6] J. Bove, M. Martinez-Vicente, M. Vila, Fighting neurodegeneration with rapamycin: mechanistic insights, Nat. Rev. Neurosci. 12 (8) (2011) 437–452.
[7] J. Li, S.G. Kim, J. Blenis, Rapamycin: one drug, many effects, Cell Metab. 19 (3) (2014) 373–379.
[8] D. Ehninger, F. Neff, K. Xie, Longevity, aging and rapamycin, Cell. Mol. Life Sci. 71 (22) (2014) 4325–4346.
[9] D.W. Lamming, L. Ye, P. Katajisto, M.D. Goncalves, M. Saitoh, D.M. Stevens, J.G. Davis, A.B. Salmon, A. Richardson, R.S. Ahima, D.A. Guertin, D.M. Sabatini, J.A. Baur, Rapamycin-induced insulin resistance is mediated by mTORC2 loss and uncoupled from longevity, Science 335 (6076) (2012) 1638–1643.
[10] T. Jiang, J.T. Yu, X.C. Zhu, M.S. Tan, H.F. Wang, L. Cao, Q.Q. Zhang, J.Q. Shi, L. Gao, H. Qin, Y.D. Zhang, L. Tan, Temsirolimus promotes autophagic clearance of amyloid-beta and provides protective effects in cellular and animal models of Alzheimer's disease, Pharmacol. Res. 81 (2014) 54–63.
[11] B. Xu, Y. Gao, S. Zhan, F. Xiong, W. Qiu, X. Qian, T. Wang, N. Wang, D. Zhang, Q. Yang, R. Wang, X. Bao, W. Dou, R. Tian, S. Meng, W.P. Gai, Y. Huang, X.X. Yan, W. Ge, C. Ma, Quantitative protein profiling of hippocampus during human aging, Neurobiol. Aging 39 (2016) 46–56.
[12] Z. Cai, G. Chen, W. He, M. Xiao, L.J. Yan, Activation of mTOR: a culprit of Alzheimer's disease? Neuropsychiatr. Dis. Treat. 11 (2015) 1015–1030.
[13] J.S. Talboom, R. Velazquez, S. Oddo, The mammalian target of rapamycin at the crossroad between cognitive aging and Alzheimer's disease, NPJ Aging Mech. Dis. 1 (2015) 15008.
[14] K. Maiese, Taking aim at Alzheimer's disease through the mammalian target of rapamycin, Ann. Med. 46 (8) (2014) 587–596.
[15] Z. Cai, L.J. Yan, Rapamycin, autophagy, and Alzheimer's disease, J. Biochem. Pharmacol. Res. 1 (2) (2013) 84–90.
[16] T.K. Ulland, W.M. Song, S.C. Huang, J.D. Ulrich, A. Sergushichev, W.L. Beatty, A.A. Loboda, Y. Zhou, N.J. Cairns, A. Kambal, E. Loginicheva, S. Gilfillan, M. Cella, H.W. Virgin, E.R. Unanue, Y. Wang, M.N. Artyomov, D.M. Holtzman, M. Colonna, TREM2 maintains microglial metabolic fitness in Alzheimer's disease, Cell 170 (4) (2017) 649–663 (e13).
[17] A.L. Lin, J.B. Jahrling, W. Zhang, N. DeRosa, V. Bakshi, P. Romero, V. Galvan, A. Richardson, Rapamycin rescues vascular, metabolic and learning deficits in apolipoprotein E4 transgenic mice with pre-symptomatic Alzheimer's disease, J. Cereb. Blood Flow Metab. 37 (1) (2017) 217–226.
[18] J.M. Schott, N.C. Fox, C. Frost, R.I. Scahill, J.C. Janssen, D. Chan, R. Jenkins, M.N. Rossor, Assessing the onset of structural change in familial Alzheimer's disease, Ann. Neurol. 53 (2) (2003) 181–188.
[19] L. Ting, R. Rad, S.P. Gygi, W. Haas, MS3 eliminates ratio distortion in isobaric multiplexed quantitative proteomics, Nat. Methods 8 (11) (2011) 937–940.
[20] Y. Chen, Y. Xie, L. Xu, S. Zhan, Y. Xiao, Y. Gao, B. Wu, W. Ge, Protein content and functional characteristics of serum-purified exosomes from patients with colorectal cancer revealed by quantitative proteomics, Int. J. Cancer 140 (4) (2017) 900–913.
[21] F. Zuo, F. Xiong, X. Wang, X. Li, R. Wang, W. Ge, X. Bao, Intrastriatal transplantation of human neural stem cells restores the impaired subventricular zone in Parkinsonian mice, Stem Cells 35 (6) (2017) 1519–1531.
[22] A. Bilkei-Gorzo, Genetic mouse models of brain ageing and Alzheimer's disease, Pharmacol. Ther. 142 (2) (2014) 244–257.
[23] A.M. Hall, E.D. Roberson, Mouse models of Alzheimer's disease, Brain Res. Bull. 88 (1) (2012) 3–12.
[24] H. Qing, G. He, P.T. Ly, C.J. Fox, M. Staufenbiel, F. Cai, Z. Zhang, S. Wei, X. Sun, C.H. Chen, W. Zhou, K. Wang, W. Song, Valproic acid inhibits Abeta production, neuritic plaque formation, and behavioral deficits in Alzheimer's disease mouse models, J. Exp. Med. 205 (12) (2008) 2781–2789.
[25] P.M. Thompson, K.M. Hayashi, G. de Zubicaray, A.L. Janke, S.E. Rose, J. Semple, D. Herman, M.S. Hong, S.S. Dittmer, D.M. Doddrell, A.W. Toga, Dynamics of gray matter loss in Alzheimer's disease, J. Neurosci. 23 (3) (2003) 994–1005.
[26] A.W. Toga, P.M. Thompson, Mapping brain asymmetry, Nat. Rev. Neurosci. 4 (1) (2003) 37–48.
[27] A. Tramutola, J.C. Triplett, F. Di Domenico, D.M. Niedowicz, M.P. Murphy, R. Coccia, M. Perluigi, D.A. Butterfield, Alteration of mTOR signaling occurs early in the progression of Alzheimer disease (AD): analysis of brain from subjects with pre-clinical AD, amnestic mild cognitive impairment and late-stage AD, J. Neurochem. 133 (5) (2015) 739–749.
[28] P. Spilman, N. Podlutskaya, M.J. Hart, J. Debnath, O. Gorostiza, D. Bredesen, A. Richardson, R. Strong, V. Galvan, Inhibition of mTOR by rapamycin abolishes cognitive deficits and reduces amyloid-beta levels in a mouse model of Alzheimer's disease, PLoS ONE 5 (4) (2010) e9979.
[29] N. Shahani, W.C. Huang, M. Varnum, D.T. Page, S. Subramaniam, Forebrain depletion of Rheb GTPase elicits spatial memory deficits in mice, Neurobiol. Aging 50 (2017) 134–143.
[30] J.T. Yu, L. Tan, J. Hardy, Apolipoprotein E in Alzheimer's disease: an update, Annu. Rev. Neurosci. 37 (2014) 79–100.
[31] V. Leduc, S. Jasmin-Belanger, J. Poirier, APOE and cholesterol homeostasis in Alzheimer's disease, Trends Mol. Med. 16 (10) (2010) 469–477.
[32] V.K. Ramanan, S.L. Risacher, K. Nho, S. Kim, S. Swaminathan, L. Shen, T.M. Foroud, H. Hakonarson, M.J. Huentelman, P.S. Aisen, R.C. Petersen, R.C. Green, C.R. Jack, R.A. Koeppe, W.J. Jagust, M.W. Weiner, A.J. Saykin, APOE and BCHE as modulators of cerebral amyloid deposition: a florbetapir PET genome-wide association study, Mol. Psychiatry 19 (3) (2014) (35135–7).
[33] G. Di Paolo, T.W. Kim, Linking lipids to Alzheimer's disease: cholesterol and beyond, Nat. Rev. Neurosci. 12 (5) (2011) 284–296.
[34] J. Habchi, S. Chia, C. Galvagnion, T.C.T. Michaels, M.M.J. Bellaiche, F.S. Ruggeri, M. Sanguanini, I. Idini, J.R. Kumita, E. Sparr, S. Linse, C.M. Dobson, T.P.J. Knowles, M. Vendruscolo, Cholesterol catalyses Abeta42 aggregation through a heterogeneous nucleation pathway in the presence of lipid membranes, Nat. Chem. 10 (6) (2018) 673–683.
[35] M.A. Wollmer, K. Sleegers, M. Ingelsson, C. Zekanowski, N. Brouwers, A. Maruszak, F. Brunner, K.D. Huynh, L. Kilander, R.M. Brundin, M. Hedlund, V. Giedraitis, A. Glaser, S. Engelborghs, P.P. De Deyn, E. Kapaki, M. Tsolaki, M. Daniilidou, D. Molyva, G.P. Paraskevas, D.R. Thal, M. Barcikowska, J. Kuznicki, L. Lannfelt, C. Van Broeckhoven, R.M. Nitsch, C. Hock, A. Papassotiropoulos, Association study of cholesterol-related genes in Alzheimer's disease, Neurogenetics 8 (3) (2007) 179–188.
[36] B. Malik, C. Fernandes, R. Killick, R. Wroe, A. Usardi, R. Williamson, S. Kellie, B.H. Anderton, C.H. Reynolds, Oligomeric amyloid-beta peptide affects the expression of genes involved in steroid and lipid metabolism in primary neurons, Neurochem. Int. 61 (3) (2012) 321–333.
[37] J.F. Oram, G. Wolfbauer, C. Tang, W.S. Davidson, J.J. Albers, An amphipathic helical region of the N-terminal barrel of phospholipid transfer protein is critical for ABCA1-dependent cholesterol efflux, J. Biol. Chem. 283 (17) (2008) 11541–11549.
[38] Y. Tong, Y. Sun, X. Tian, T. Zhou, H. Wang, T. Zhang, R. Zhan, L. Zhao, B. Kuerban, Z. Li, Q. Wang, Y. Jin, D. Fan, X. Guo, H. Han, S. Qin, D. Chui, Phospholipid transfer protein (PLTP) deficiency accelerates memory dysfunction through altering amyloid precursor protein (APP) processing in a mouse model of Alzheimer's disease, Hum. Mol. Genet. 24 (19) (2015) 5388–5403.
[39] S. Vuletic, L.W. Jin, S.M. Marcovina, E.R. Peskind, T. Moller, J.J. Albers, Widespread distribution of PLTP in human CNS: evidence for PLTP synthesis by glia and neurons, and increased levels in Alzheimer's disease, J. Lipid Res. 44 (6) (2003) 1113–1123.
[40] Q. Ding, W.R. Markesbery, Q. Chen, F. Li, J.N. Keller, Ribosome dysfunction is an early event in Alzheimer's disease, J. Neurosci. 25 (40) (2005) 9171–9175.
[41] L. Rasmussen, R.W. de Labio, G.A. Viani, E. Chen, J. Villares, P.H. Bertolucci, T.S. Minett, G. Turecki, D. Cecyre, S.A. Drigo, M.C. Smith, S.L. Payao, Differential expression of ribosomal genes in brain and blood of Alzheimer's disease patients, Curr. Alzheimer Res. 12 (10) (2015) 984–989.
[42] A. Caccamo, C. Branca, J.S. Talboom, D.M. Shaw, D. Turner, L. Ma, A. Messina, Z. Huang, J. Wu, S. Oddo, Reducing ribosomal protein S6 kinase 1 expression improves spatial memory and synaptic plasticity in a mouse model of Alzheimer's disease, J. Neurosci. 35 (41) (2015) 14042–14056.
[43] V. Iadevaia, R. Liu, C.G. Proud, mTORC1 signaling controls multiple steps in ribosome biogenesis, Semin. Cell Dev. Biol. 36 (2014) 113–120.
[44] V. Zinzalla, D. Stracka, W. Oppliger, M.N. Hall, Activation of mTORC2 by association with the ribosome, Cell 144 (5) (2011) 757–768.